Air mass classification during the INDOEX R/V Ronald Brown cruise using measurements of nonmethane hydrocarbons, CH 4 , CO 2 , CO, 14 CO, and δ 18 O(CO)

Jens Mühle, Andreas Zahn, Carl A. M. Brenninkmeijer, Valérie Gros, Paul J. Crutzen

Air mass classification during the INDOEX R/V *Ronald Brown* cruise using measurements of nonmethane hydrocarbons, CH_4, CO_2, CO, ^{14}CO, and $\delta^{18}O(CO)$

Jens Mühle, Andreas Zahn, Carl A. M. Brenninkmeijer, Valérie Gros, and Paul J. Crutzen

Air Chemistry Division, Max Planck Institute for Chemistry, Mainz, Germany

Received 6 October 2000; revised 7 March 2001; accepted 2 April 2001; published 6 September 2002.

[1] During the Indian Ocean Experiment (INDOEX) in February-March 1999 the impact of continental outflow to the Indian Ocean was analyzed. On board the R/V *Ronald Brown* altogether 93 air samples were taken for analysis of nonmethane hydrocarbons (NMHC), methane (CH_4), carbon dioxide (CO_2), carbon monoxide (CO), and the $^{14}C/^{12}C$ and $^{18}O/^{16}O$ isotope ratios of CO. Five types of air masses differing in origin, degree of pollution, and chemical age were identified based on back trajectory analyses and the trace gas data, supported by continuous CO and ozone (O_3) observations from other investigators. The Indian Ocean was found to be frequently affected by nearby emissions from the Indian subcontinent and Indochina, but the strongest pollution event (characterized inter alia by high mixing ratios of medium- and long-lived NMHC) was due to long-range advection from the extratropical northern hemisphere. Carbon monoxide 14 showing a distinct meridional profile unequivocally confirms this remote impact. The ratio acetylene/CO was found to be often inadequate as a measure for atmospheric processing, the integrated influence of OH chemistry and mixing. Our data suggest that the influence from fresh continental pollution was less pronounced along the INDOEX R/V *Ronald Brown* cruise compared to observations made during other tropical campaigns, such as the Pacific Exploratory Mission-West B in the Pacific Ocean. *Index Terms:* 9340 Information Related to Geographic Region: Indian Ocean; 0368 Atmospheric Composition and Structure: Troposphere—constituent transport and chemistry; 1040 Geochemistry: Isotopic composition/chemistry; 3307 Meteorology and Atmospheric Dynamics: Boundary layer processes; 3374 Meteorology and Atmospheric Dynamics: Tropical meteorology; *Keywords:* INDOEX, Indian Ocean, NMHC, isotopes, air mass classification, long-range transport

Citation: Mühle, J., A. Zahn, C. A. M. Brenninkmeijer, V. Gros, and P. J. Crutzen, Air mass classification during the INDOEX R/V *Ronald Brown* cruise using measurements of nonmethane hydrocarbons, CH_4, CO_2, CO, ^{14}CO, and $\delta^{18}O(CO)$, *J. Geophys. Res.*, *107*(D19), 8021, doi: 10.1029/2001JD000730, 2002.

1. Introduction

[2] The fast industrialization of countries in Asia, in particular India and China, comes along with large and rapidly increasing emissions of various pollutants to the atmosphere. Especially during the winter (northeast) monsoon (January-March), the Indian Ocean becomes a unique region where the temporal and spatial development of emissions from the Indian subcontinent and Southeast Asia can be studied. This particularly implies the mixing of continental outflow of pollutants and aerosols with pristine SH air masses by cross-equatorial monsoonal flow into the Intertropical Convergence Zone (ITCZ). A major intention of the Indian Ocean Experiment (INDOEX) was to improve the understanding of the interactions between aerosols, clouds, chemistry, and climate. Special emphasis was on the radiative forcing effect of anthropogenic aerosols and on the role of the ITCZ in interhemispheric transport of trace gases and aerosols. The intensive field campaign of INDOEX took place in February-March 1999 and involved several aircrafts, ships, and island stations in the Indian Ocean region. A main goal of the National Oceanic and Atmospheric Administration (NOAA) research vessel *Ronald Brown* as one of the platforms was to characterize the trace gas and aerosol composition of outflow from the Indian subcontinent and its chemical processing over the Indian Ocean.

[3] Prior to INDOEX, only sparse trace gas observations have been carried out in the Indian Ocean such as the second Soviet American Gases and Aerosols campaign (SAGA II) in 1987 [*Butler et al.*, 1988; *Arlander et al.*, 1990; *Johnson et al.*, 1990] or the Joint Global Ocean Flux Study (JGOFS) during which nitrous oxide (N_2O), CH_4, and CO_2 were measured [*Bange et al.*, 1996, 1998; *Goyet et al.*, 1998; *Upstill-Goddard et al.*, 1999, and references therein]. More recent studies in this region (predominantly on tropospheric O_3) [*Baldy et al.*, 1996; *Gros et al.*, 1998; *de Laat et al.*, 1999; *Taupin et al.*, 1999] point to considerable impact of continental pollutants, even at very

Paper number 2001JD000730.
0148-0227/02/2001JD000730

Table 1. Rate Constants and Lifetimes of Selected Trace Gases Under Typical Midlatitude and Tropical Conditions

Compound	Main Sources	K_{OH} at 298 K, cm^3 $molecule^{-1}$ s^{-1}	OH Photochemical Lifetimes, days	
			$[OH]_{midlatitudes}$, 5×10^5 molecule cm^{-3}	$[OH]_{tropics}$, 3×10^6 molecule cm^{-3}
Methane[a, b]	industrial/natural gas loss/wetlands/ ruminants/biomass burning	6.34×10^{-15}[c]	3650 (10 years)	608 (1.7 years)
Ethane[a, d]	natural gas loss/biomass burning/	2.40×10^{-13}[c]	96.5	16.1
Propane[a]	vegetation	1.09×10^{-12}[c]	21.2	3.5
Acetylene[a]	industrial/biomass burning	7.47×10^{-13}[c]	31.0[e] (30.3[f])	5.2[e] (5.2[f])
Carbon monoxide[a, b]	industrial/biomass burning/hydrocarbons + OH	$(1.5 + 0.9\ P_{atm}) \times 10^{-13}$[c]	96.5(1 atm)	16.1(1 atm)

[a][*Hough*, 1991].
[b][*IPCC*, 1995].
[c][*DeMore et al.*, 1997].
[d][*Rudolph*, 1995].
[e]Here 25 ppb O_3.
[f]Here 30 ppb O_3.

remote stations. This finding was confirmed by shipborne trace gas and aerosol measurements in 1995 by *Rhoads et al.* [1997], as part of the World Ocean Circulation Experiment (WOCE), as well as by CO, CH_4, O_3, and aerosol measurements by *Lal et al.* [1998]. A compilation of further pre-INDOEX research can be found in the works of *Rhoads et al.* [1997] and *Mitra* [1999], and at http://www-indoex.ucsd.edu/databyevent.html. Besides these campaigns, the NOAA/Climate Monitoring and Diagnostics Laboratory (CMDL) monitors CO, CH_4, and CO_2 at several stations in the Indian Ocean [*Novelli et al.*, 1995, 1998].

[4] Purpose of the present paper is to characterize the air masses encountered by the R/V *Ronald Brown* by applying a powerful set of contrasting tracers, in particular nonmethane hydrocarbons. The detected trace gases (NMHC, CH_4, CO, CO_2, N_2O, and SF_6) do have lifetimes between days (e.g., propane) and years (e.g., CH_4) and diverse sources, e.g., biogenic, oceanic, and anthropogenic (see Table 1).

[5] Although NMHC play a key role in atmospheric chemistry, particularly with respect to photochemical O_3 production, only little information is available on their fate in the Indian Ocean area, especially during the INDOEX conditions, i.e., the northern Indian Ocean during the winter monsoon. General information on the global distribution and seasonality of NMHC and their fate in the atmosphere is given by *Singh and Zimmerman* [1992] and *Rudolph* [1995] (additional details are given by *Rudolph et al.* [1996] and *Bonsang and Boissard* [1999]). Even pristine areas of the southern hemisphere (SH) are influenced by long-range transport of long-lived NMHC emitted by continental sources [e.g., *Touaty et al.*, 1996; *Saito et al.*, 2000], while short-lived NMHC are determined by emissions from the ocean [e.g., *Bonsang et al.*, 1993; *Plass-Dülmer et al.*, 1995; *Lewis et al.*, 1999].

[6] In addition to the mixing ratio of CO, its $C^{18}O$ (stable) and ^{14}CO (radioactive) isotope composition was measured. $\delta^{18}O(CO)$ expresses the isotope ratio $^{18}O/^{16}O$ in CO relative to the Vienna-Standard Mean Ocean Water (V-SMOW) standard in per mil. High $\delta^{18}O(CO)$ values (~23‰) are associated with fossil fuel combustion, whereas biomass burning derived CO is less enriched (15 to 18‰), and photochemically generated CO is assumed to show $\delta^{18}O(CO)$ of ~0‰. Note that isotope fractionation during oxidation by OH yields progressive depletion in $\delta^{18}O(CO)$. Atmospheric ^{14}CO (given in molecules per cm^3 air STP) is mainly produced by cosmic rays, primarily in the midlatitude and high-latitude upper troposphere and lower stratosphere. It has also a small biogenic contribution ("recycled CO") from the incomplete oxidation of organic matter containing ^{14}C from CO_2 assimilation. The main sink of ^{14}CO is, as for CO, oxidation by OH. Note, that CO from fossil fuel combustion is free of ^{14}CO. Observed isotopic composition of CO thus reflects both the signature of the different sources as well as fractionation and dilution occurred during transport [*Brenninkmeijer et al.*, 1999; *Jöckel*, 2000, and references therein].

[7] After a brief description about the analytical techniques applied (section 2), a short overview about the meteorological conditions during INDEX is given (section 3). Thereafter the observed trace gas time series are analyzed (section 4), and the intersected air masses are classified based upon back trajectory analyses and the trace gas data (section 4.1). The influence of long-range transport on the observed trace gas variability is discussed (section 4.2), and the meaning of the acetylene/CO ratio is evaluated (section 4.3). Finally, the entire data set is compared with previous results (section 5), and the conclusions are given (section 6).

2. Experimental Techniques

2.1. Air Sampling and Analyzed Compounds

[8] Ninety-three air samples (sample locations in Figure 1) were collected in 2.5 L electropolished stainless steel canisters fitted with metal bellow valves (Nupro SS-4H). Using a metal bellows pump (Parker, MB-158-E, operation temperature below 65°C), air was sucked from the top of a bow tower (10 m height) via a 25 m stainless steel tube (ID: 4 mm) through an ice water cold trap (0°C) to reduce the water vapor mixing ratio to ~0.6%. After flushing several times, the canisters were filled to a final pressure of 3.7 bar leading to sample sizes of ~9 L (STP) each. With exception of the transport time (~6 days) to the laboratory (MPI-C, Mainz, Germany) the canisters were kept at −18°C. Twelve hours before gas chromatographic (GC) analysis of NMHC, CH_4, CO_2, SF_6, and N_2O the canisters were stored at ambient temperature.

[9] For measuring CO and its isotope ratios ($^{18}O/^{16}O$, $^{14}C/^{12}C$), fifteen 600 L (STP) air samples (sample locations in Figure 1) were also collected from the bow tower (via a ½ inch

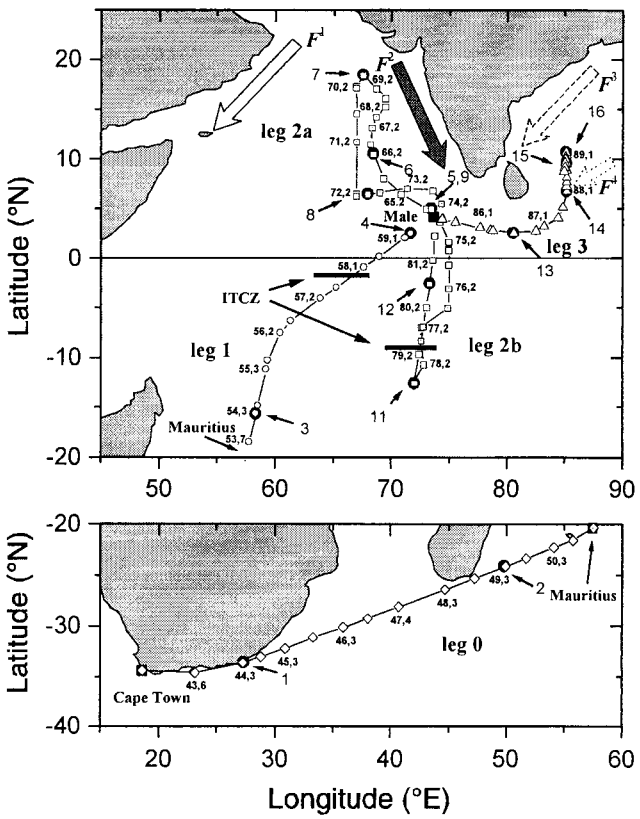

Figure 1. Cruise track of the R/V *Ronald Brown* during INDOEX (11 February to 30 March 1999, day of year (DOY) 42–89), showing the locations of 9 L (STP) air samples (open symbols) and 600 L air samples for isotopic analyses of CO (solid circles, labeled 1–9 and 11–16). DOY are noted as small numbers. The four typical airflows over the Indian Ocean are labeled as F^1, F^2, F^3, and F^4, and the positions of the strong convergence zones are marked with ITCZ (see section 3). For a better visualization, leg 1 (open circles, 22–28 February, DOY 53–59), leg 2a (open squares, 5–15 March, DOY 64–74), leg 2b (open squares, 16–22 March, DOY 78–81), and leg 3 (open triangles, 26–30 March DOY 85–89) are shown in the top part, and leg 0 (open diamonds, 12–19 February, DOY 43–50) is shown in the lower part. For legs 0 and 1, CH_4, CO_2, N_2O, SF_6, and isotopic composition of CO were analyzed. For legs 2 and 3, additionally NMHC were measured.

PFA tube) by using 5 L aluminum cylinders (Scott-Marrin Inc., Riverside California). An improved version of the clean air compressor described by *Mak and Brenninkmeijer* [1994] was used. The flushing and filling procedure took ~60 min.

[10] On the samples collected during the pre-INDOEX leg 0 (12–19 February 1999, day of year (DOY) 43–50) and INDOEX leg 1 (22–28 February 1999, DOY 53–59), analysis of CH_4, CO (including its isotopic composition), CO_2, N_2O, and SF_6 were performed. For leg 2 (5–22 March 1999, DOY 64–81) and leg 3 (26–30 March 1999, DOY 85–89), additionally NMHC were analyzed. Owing to the limited additional information derived, the N_2O and SF_6 data are not assessed in detail.

2.2. Laboratory-Based NMHC Measurements

[11] A general overview about gas chromatographic techniques for measuring atmospheric trace species is given by *Camel and Caude* [1995] and *Helmig* [1999]. Here the 59 samples from leg 2 and 3 were separated on a 50 m, ID: 0.32 mm, 5 μm Al_2O_3/KCl porous layer open tubular (PLOT) column (Chrompack) by using a gas chromatograph (Hewlett-Packard, HP 6890) with subambient temperature capability connected to a quadrupole mass spectrometer (HP 5973). Sample aliquots of 350 ml (STP) air initially passed two scavenger traps (length: 11 cm, ID: 0.7 cm) filled with anhydrous lithium hydroxide (Merck) and anhydrous magnesium perchlorate (Fluka) to remove CO_2 and H_2O. Tests indicated insignificant influence of the scavenger traps on the measured NMHC [*Matuška et al.,* 1986; *Habram et al.*, 1998; *Kurdziel*, 1998; *Rasmussen et al.*, 1996; *Lewis et al.*, 1999]. The condensible compounds (encompassing the NMHC) were cryogenically concentrated in a stainless steel microtrap (−170°C, length: 30 cm, ID: 0.03 inch), packed along 10 cm with porous silica beads (Unibeads 1S, 60/80 mesh, Alltech) over 8 min at a flow of 45 mL min^{-1} (controlled by a mass flow controller, MKS Type 1179A). Similar techniques were used by *Singh et al.* [1988], *Rudolph et al.* [1990], *Doskey* [1991], *Doskey et al.* [1992], and *Mitra and Yun* [1993]. During trapping, the sample trap was connected to an evacuated gas reservoir (2.54 L) to determine the sample size volumetrically. Afterwards, the trap was flushed with helium for 5 min to remove traces of oxygen and nitrogen.

[12] The retained compounds were desorbed from the trap by heating from the initial −170°C to +150°C in ~3 s [*Mitra and Yun,* 1993] and introduced into the analytical column. The GC column was held at 10°C for 11 min and subsequently heated at 5°C min^{-1} to 200°C and maintained at 200°C for another 10 min. Helium 6.0 further purified by a three-stage gas purifier and a cryogenic trap (filled with activated charcoal) at liquid nitrogen temperature was used as carrier and flushing gas. The initial column head gauge pressure was 0.81 bar at 10°C, increased during heat up of the column to maintain a constant flow. All connections were made of compression type stainless steel fittings. The sample path and the inlet line are of stainless steel and silcosteel (Restek Corp.), respectively, held at 60°C to avoid condensation of species of low vapor pressure.

[13] The mass spectrometric detector was operated in Single-Ion Monitoring (SIM) mode to enhance sensitivity compared to SCAN mode. For each compound, *m/z* values were carefully chosen with respect to background, coeluting compounds and sensitivity. One characteristic *m/z* value per compound was used to derive its concentration, and up to three other *m/z* values were used to check identity and to cross-check correct quantification for the (unlikely) case of coelution. Most of the analyzed compounds were clearly separated, except of acetylene (C_2H_2) and butane. Each chromatogram was integrated by a MSD Software (Hewlett-Packard) and checked manually. The mass spectrometer was tuned weekly. Analyses have been made for light alkanes such as ethane (27), propane (29), butane (43), iso-butane (43), pentane (43), iso-pentane (43), light alkenes such as ethene (27), propene (41), 1-butene (41), trans-2-butene (41), cis-2-butene (41), and acetylene (26); the *m/z* values used for quantification are in parenthesis.

[14] A calibration following each fourth sample was made by aliquoting different volumes of a standard gas mixture (1 to 10 mL) leading in a linear calibration line ($r^2 \geq 0.99$) for each compound. The detection limits (3 σ variation of a blank sample) were 0.2 to 6.8 pptv (ethane, propane, butane, iso-butane, pentane, and iso-pentane), 0.2 to 16.1 pptv (ethene, propene, 1-butene, trans-2-butene, cis-2-butene), and 14 to 26 pptv (acetylene), and the precision was 5 to 10%.

[15] A 30 compound reference standard from the National

Physical Laboratory (Teddington, United Kingdom) with a certified uncertainty range of 1.2 to 2.2% (95% confidence limit) for each compounds was used for absolute calibration. The calibration is currently cross-checked by measuring samples used during the Nonmethane Hydrocarbon Intercomparison Experiment (NOMHICE) [*Apel and Calvert*, 1994; *Apel et al.*, 1994, 1999]. First comparisons show an agreement within ~20% for all species addressed in this paper.

[16] Long-term laboratory tests (11 months) have revealed significant formation of alkenes in the sample canisters, a problem already discussed by *Donahue and Prinn* [1993]. Even in sample canisters kept at −18°C we detected production rates of ~4 ppt $month^{-1}$ for ethene and ~2 ppt $month^{-1}$ for propene. No significant changes for alkanes and acetylene were noticed. However, it is worth mentioning that the measured ethene (28 to 128 ppt) and propene (10 to 50 ppt) mixing ratios were highly correlated. This ethene to propene slope of 2.7 ppt/ppt ($r^2 = 0.90$) stands in agreement with values determined by on-line measurements on the Atlantic Ocean of 2.5 in the SH and 2.9 in the NH [*Rudolph and Johnen*, 1990]. As we are not able to precisely determine how much the INDOEX alkene data were affected by storage artifacts, they are not further discussed.

2.3. Measurement of Long-lived Trace Gases, CO, $\delta^{18}O(CO)$, and ^{14}CO

[17] Analyses of CH_4, CO_2, N_2O, and SF_6 were made with an automated GC system (Hewlett Packard, HP 6890a) with flame ionization detector (FID), electron capture detector (ECD), and a HP 5790 nickel catalyst for reduction of CO_2 to CH_4 (set up by Atmospheric Environmental Service, Canada) [*Bräunlich,* 2000]. The absolute uncertainty of the measurements is 3 ppb for CH_4, 0.3 ppm for CO_2, 2 ppb for N_2O, and 0.1 ppt for SF_6. CH_4, CO_2, and N_2O are given versus the NOAA scale, SF_6 is calibrated on a GC system, described by *Maiss et al.* [1996].

[18] The 600 L (STP) samples are analyzed for the concentration of CO and its isotopic composition ($\delta^{18}O(CO)$, ^{14}CO). The CO concentration is derived with an absolute measurement method, based on the conversion of CO into CO_2 and subsequent volumetric measurement of the derived CO_2. The $^{18}O/^{16}O$ isotope ratio of CO is determined by mass spectrometry, and the ^{14}C content is analyzed via accelerator mass spectrometry [see *Brenninkmeijer*, 1993; *Brenninkmeijer et al.*, 1999, 2001].

[19] The continuous measurements of CO and O_3 [*Stehr et al.*, 2002] were done with a TECO 48 CO and a TECO 49 O_3 analyzer (Thermo Environmental Instruments Inc., Franklin, Massachusetts), respectively, here given as 30 min averages. The agreement between continuous CO and laboratory based CO measurements on the 600 L samples is generally better than 5 ppb.

3. Meteorology During INDOEX

[20] A short overview about the meteorological conditions encountered along the ship track and the major near-surface airflows over the Indian Ocean is given here.

3.1. Dominating Airflows

[21] A 10 year climatological study of the Indian Ocean presented in the meteorology overview by *Verver et al.* [2001] pointed out that four prevailing airflows (F^1, F^2, F^3, F^4) advect (mainly continental) air to the Indian Ocean (Figure 1): F^1, northeast (NE) trades over the western Arabian Sea, F^2, NE-NW flow along the west coast of India, F^3, NE trades over the west Bay of Bengal, and F^4, NE flow from Southeast Asia. They are mainly driven by pressure difference developing between subtropical high-pressure systems stretched along 20°N (from Arabia to Southeast Asia) and organized clusters of convective systems around the equator (15°S to 10°N). The strength of the four airflows fluctuates on a day-to-day basis, strongly modulated by the actual weather regime.

[22] During INDOEX, F^1 was generally the most active channel, but it was west of the region examined and thus was never passed by the *Ronald Brown.* F^3 was very active up to 6 March (DOY 65) and was most likely responsible for the polluted air masses probed at ±2°N, 70°E during the end of leg 1 (27–28 February, DOY 58–59) and at 5–6°N, 70–73°E the beginning of leg 2a (5–6, March, DOY 64–65). Exceptionally, during the major part of leg 2 (7–22 March, DOY 66–81) and the entire leg 3 (26–30 March, DOY 85–89) the two eastern channels F^3 and F^4 were nearly absent, but channel F^2 was (in contrast to February) quite active. These anomalies had crucial consequences for the trace gas composition probed during leg 2 and 3: (1) during 9–16 March (DOY 68–75), F^2 brought midlatitude air (from 20°–45°N) to the measurement site at 2°–19°N, 68°–75°E (Arabian Sea), and (2) during leg 3 (taken place in the Bay of Bengal) polluted but aged continental air (earlier imported by F^3 and F^4) was intersected.

3.2. Location of the Intertropical Convergence Zone (ITCZ)

[23] In February-March 1999 the ITCZ was broken into two convergence zones (CZ) [*Verver et al.*, 2001]. The northern CZ was more active in February at 1°S–7°N, and the southern CZ became dominant in March between 10°S, 60°E and 5°S, 100°E, along the region of highest sea surface temperatures of 28°–29°C. The transition zone between SH air and NH air, unambiguously identified by a sharp jump in several trace species, such as CO from ≤65 ppb (SH) to ≥95 ppb (NH), coincided with the northern CZ on 26 February (end of DOY 57) at ~1°S and with the southern CZ encountered on 19–20 March (DOY 78–79) south of 9°S (Figure 1).

4. Results and Discussion

[24] As seen in Figure 1, the 93 sample locations are quite homogeneously distributed over the various legs with an average sample frequency of 2.3 canisters (9 L STP) per day. The time series of medium- and longer-lived trace gases show substantial variability (Figure 2). The highest concentrations were observed on 10 March (DOY 69), except for CO that peaked on 6 March (DOY 64.9). All trace gases minimized during 19–20 March (DOY 78–79) as the ship was south of the chemical ITCZ. These trace gas changes are expected to reflect predominantly the different origin of the air masses since the transport timescale (about 1 week) is shorter than the chemical lifetime for most of the shown trace gases. To support this claim, back trajectories were calculated, and the inferred air mass classification was subsequently compared with the trace gas signature observed in the different types of air masses.

4.1. Trajectory and Trace Gas Composition Based Air Mass Classification

[25] For each individual sampling location, diabatic 3-D 5-day back trajectories (ending at 950 hPa) were calculated

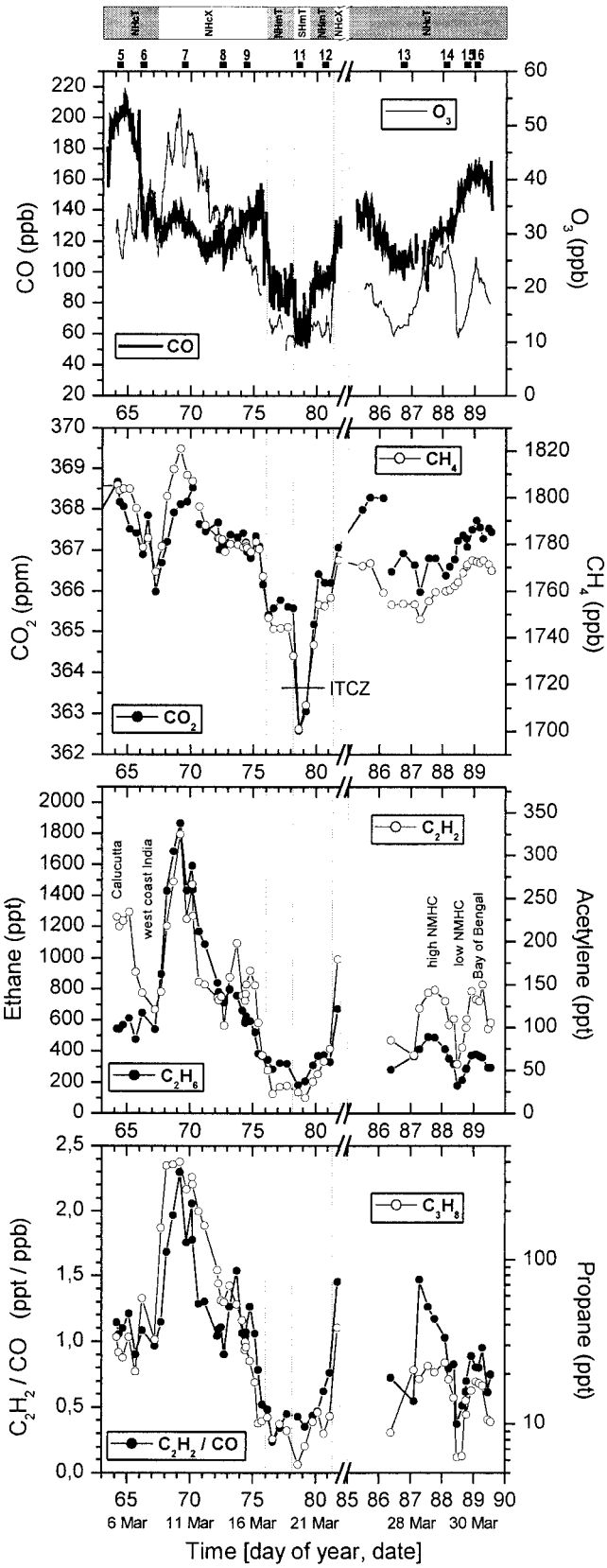

Figure 2a. Times series of trace gas mixing ratios (leg 2 and leg 3). The transitions between the different air masses (SHmT, NHmT, NHcT, and NHcX) are indicated by vertical lines. Bold numbers show location of 600 L air samples for isotopic analyses of carbon monoxide. The crossing of the strong southern CZ is marked by ITCZ.

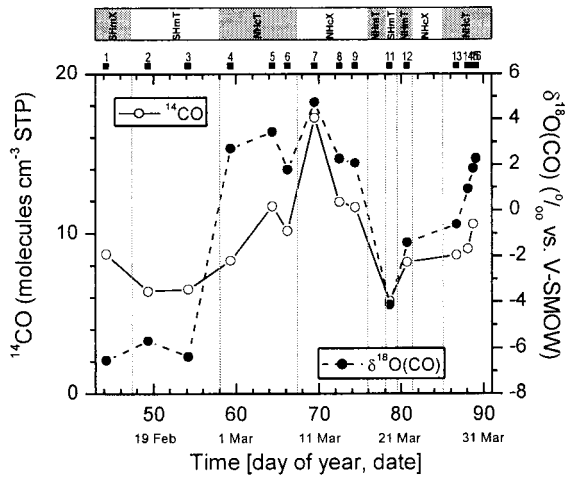

Figure 2b. Times series of ^{14}CO and $\delta^{18}O(CO)$ (legs 0 to 3). The transitions between the different air masses (SHmX, SHmT, NHmT, NHcT, and NHcX) are indicated by vertical lines. Carbon monoxide 14 sample 16 was lost during accelerator mass spectrometry. Note the time series is enlarged compared to Figure 2a to show all results of isotopic measurements.

with the Hybrid Single-Particle Langrangian Integrated Trajectories (HYSPLIT) program [*Draxler and Hess*, 1998] to estimate the origin of the probed air masses. On the basis of the air mass classification proposed by *Rhoads et al.* [1997] and further specified by altogether five types of W. P. Ball et al. (unpublished manuscript, 2002), air masses were encountered during the INDOEX R/V *Ronald Brown* cruise. During legs 2 and 3, four air mass types were intersected: Northern Hemisphere continental tropical (NHcT), Northern Hemisphere continental extratropical (NHcX), Northern Hemisphere marine tropical (NHmT), and Southern Hemisphere marine tropical (SHmT). During legs 0 and 1, also Southern Hemisphere maritime extratropical (SHmX) air was temporarily intercepted. The identification of the individual types of air masses was done with respect to the starting area of the back trajectories by applying the following rules:

[26] NHcX air parcels originated from the continental extratropics (mainly from Arabian Peninsula, Middle East, and Europe) and were advected to the sampling site via the airflow F^2 south-eastward along the coast of Pakistan and the Indian west coast. Trajectories that started over the Indian subcontinent were attributed to NHcT air. They reached the Indian Ocean mostly via F^3 (e.g., by passing the Bay of Bengal) and to a minor degree via F^2. Air parcels without contact to landmasses for more than 5 days were classified as NHmT or SHmT according to their origin (NH or SH). Air masses that originated from the zonal westerly flow of the southern Indian Ocean (south of 30 °S) were classified as SHmX air.

[27] Because of the known uncertainties of back trajectories [*Stohl*, 1998], in particular in areas with weak winds and near convective zones, daily stream fields (available for legs 0, 1, and 2 at http://www.joss.ucar.edu/indoex/catalog/) were additionally assessed to better distinguish between SHmT and NHmT air.

[28] The five types of air masses are assumed to show quite contrasting trace gas compositions, due to their advection

Table 2. Mixing Ratios (Mean and 1 σ Variation) for the Five Types of Air Masses Encountered by the R/V *Ronald Brown* During INDOEX

	SHmX	SHmT	NHmT	NHcT	NHcX
Day of year	43.5–47.4	48.3–57.6 78.6–79.2	76.2–77.7 79.8–81.2	58.1–67.2 85.5–89.5	67.7–75.7 81.8
Number of samples[a]	9 (0)	18 (2)	9 (8)	33 (25)	24 (24)
CH_4, ppb	1688.8 ± 1.2	1694.8 ± 7.5	1746.1 ± 8.2	1774.0 ± 17.7	1787.3 ± 14.5
CO_2, ppm	360.9 ± 0.3	361.2 ± 0.9	365.8 ± 0.4	367.1 ± 0.8	367.4 ± 0.7
N_2O, ppb	312.5 ± 0.1	312.8 ± 0.3	314.2 ± 0.4	314.4 ± 0.5	314.3 ± 0.5
SF_6, ppt	4.082 ± 0.018	4.126 ± 0.033	4.312 ± 0.034	4.329 ± 0.059	4.384 ± 0.040
Ethane, ppt	no data	193.5 ± 17.9	331.8 ± 30.1	402.9 ± 125.1	926.9 ± 429.0
Propane, ppt	no data	6.5 ± 1.2	10.0 ± 1.3	20.2 ± 11.0	132.5 ± 133.9
Acetylene, ppt	no data	21.1 ± 4.6	44.2 ± 17.3	133.2 ± 48.8	169.3 ± 59.8
C_2H_2/CO, ppt/ppb	no data	0.39 ± 0.06	0.48 ± 0.16	0.89 ± 0.26	1.31 ± 0.43
CO,[b] ppb	no data	55.8 ± 9.0	92.8 ± 6.9	154.7 ± 30.8	127.1 ± 9.2
O_3,[c] ppb	no data	11.8 ± 2.6	12.5 ± 1.3	24.4 ± 7.9	35.8 ± 8.6
Number of samples	1	3	1	7[d]	3
^{14}CO, cm^{-3} air ^{STP}	8.70	6.20 ± 0.40	8.19	9.72 ± 1.30	13.59 ± 3.15
$\delta^{18}O(CO)$, ‰	−6.56	−5.41 ± 1.14	−1.41	1.76 ± 1.31	3.02 ± 1.50

[a]Number of NMHC measurements (only made for legs 2 and 3) are given in parentheses.
[b]CO with courtesy of J. Johnson (continuous measurements [*Stehr et al.*, 2002].
[c]O_3 with courtesy of J. Stehr (continuous measurements [*Stehr et al.*, 2002]).
[d]Carbon monoxide 14 sample 16 was lost during accelerator mass spectrometry.

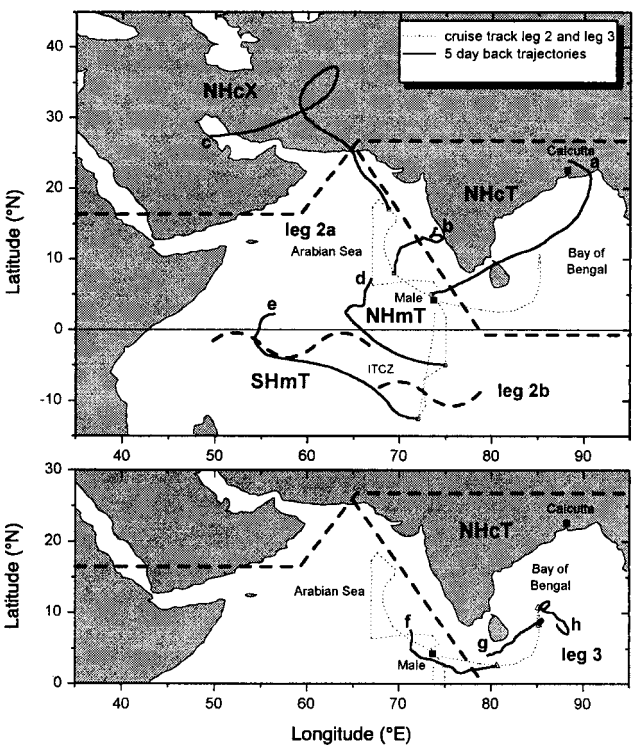

Figure 3. Air mass classification (leg 2 and leg 3) with typical 5-day back trajectories (ending at 950 hPa): Northern Hemisphere continental tropical (NHcT, trajectories a, b, f, g, h), Northern Hemisphere continental extratropical (NHcX, trajectory c), Northern Hemisphere marine tropical (NHmT, trajectory d), and Southern Hemisphere marine tropical (SHmT, trajectory e). On the basis of this air mass classification the typical source regions are indicated by dashed lines. The variable location of the chemical ITCZ and thus the distinction between SHmT and NHmT is shown by a waved, dashed line. For a better visualization, leg 2 (top part) and leg 3 (lower part) are separated.

from/over very different trace gas source regions. To confirm this claim, trace gas mean values and their variance in the five air mass types were inspected. For legs 0, 1, and 2 the assumption is excellently confirmed (see Table 2 and the following discussion), but for leg 3 (that only covered 5 days of measurements) some differences arose, as discussed later on. Figure 3 shows the source regions of the different types of air masses with typical 5-day back trajectories, which are described in detail as follows.

4.1.1. Leg 2

[29] NHmT (DOY 76.2–77.7 and 79.8–81.2) and SHmT (DOY 78.6–79.2) maritime air masses stayed over the Indian Ocean for at least 5 days (see example trajectories d and e in Figure 3), and the concentrations of most compounds were correspondingly low (Table 2). The transition from NHmT air to SHmT air (DOY 78–79), i.e., the crossing of the chemical ITCZ, is manifested by a distinct drop of all trace gases except O_3. Although the transition between SHmT and NHmT during leg 2b is not illustrated by the back trajectories, it is seen from the stream fields that the ship was under strong influence of southern hemispheric air in the period classified as SHmT. The SHmT air probed during leg 0 (between Mauritius and the equator) were of more pristine origin than during leg 2 (DOY 78–79), demonstrated inter alia by the lower $\delta^{18}O(CO)$ values.

[30] In NHcX (DOY 67.7–75.7) air masses most trace gases such as several hydrocarbons, CH_4, O_3, $\delta^{18}O(CO)$, and ^{14}CO showed the highest concentrations detected during INDOEX. They originated from the midlatitude free troposphere (<550 hPa) (Arabian Peninsula, Middle East, and Europe), only subsided near the coastline (trajectory c), and reached the sampling locations via F^2. Up to 1866 ppt ethane, 325 ppt acetylene, 1821 ppb CH_4, 53 ppb O_3 (DOY 69.2), 4.8‰ $\delta^{18}O(CO)$, and 17.2 ^{14}CO molecules cm^{-3} (STP, DOY 69.7) were observed (Figure 2). This event was not due to biomass burning, since the typical marker acetonitrile minimized [*Wisthaler et al.*, 2002]. Most trace gas mixing ratios decreased while the dis-

Table 3. Mixing Ratios (Mean and 1 σ Variation) for Air Masses Classified as NHcT

	Leg 2		Leg 3		
Specific Event	Calcutta	West Coast India	High NMHC	Low NMHC	Bay of Bengal
Day of year	64.2–65.2	65.7–67.2	87.3–88.1	88.5–88.6	88.9–89.3
Number of samples[a]	4 (4)	4 (3)	4 (4)	2 (2)	4 (4)
CH_4, ppb	1804.0 ± 1.0	1781.2 ± 11.3	1755.7 ± 5.6	1765.7 ± 2.8	1772.5 ± 0.5
CO_2, ppm	368.1 ± 0.5	367.0 ± 0.8	366.5 ± 0.4	367.3 ± 0.1	367.5 ± 0.2
N_2O, ppb	315.4 ± 0.3	315.1 ± 0.4	314.0 ± 0.3	314.0 ± 0.0	314.4 ± 0.1
SF_6, ppt	4.412 ± 0.019	4.359 ± 0.053	4.333 ± 0.062	4.275 ± 0.065	4.305 ± 0.062
Ethane, ppt	565.6 ± 32.2	544.2 ± 86.6	450.3 ± 43.7	195.4 ± 24.6	370.3 ± 9.8
Propane, ppt	29.7 ± 4.3	36.9 ± 18.9	21.2 ± 2.1	6.3 ± 0.1	17.1 ± 0.9
Acetylene, ppt	225.7 ± 7.1	141.8 ± 21.9	134.0 ± 9.4	66.6 ± 13.7	138.5 ± 9.0
C_2H_2/CO, ppt/ppb	1.13 ± 0.07	0.98 ± 0.09	1.23 ± 0.20	0.44 ± 0.08	0.86 ± 0.14
CO,[b] ppb	203.1 ± 4.8	146.1 ± 18.9	119.0 ± 9.8	151.2 ± 2.6	162.9 ± 3.0
O_3,[c] ppb	30.1 ± 3.4	35.9 ± 3.0	24.7 ± 0.5	12.2 ± 0.9	22.4 ± 1.5
Number of samples	1	1	1	-	1 (0)[d]
^{14}CO, cm^{-3} air ^{STP}	11.68	10.14	9.00	-	-
$\delta^{18}O(CO)$, ‰	3.45	1.78	0.93	-	2.26

[a]Number of NMHC measurements are given in parentheses.
[b]CO with courtesy of J. Johnson (continuous measurements [*Stehr et al.*, 2002]).
[c]O_3 with courtesy of J. Stehr (continuous measurements [*Stehr et al.*, 2002]).
[d]Carbon monoxide 14 sample 16 was lost during accelerator mass spectrometry.

tance to the coast lengthens (~DOY 70–75.7). The isolated acetylene and CO peaks (DOY 73–75) were probably related to input from combustion processes [*Wisthaler et al.*, 2002], supported by the trajectories which were tangent to the coastline. Compared to the relative uniform trace gas composition in the maritime regimes and the characteristic air mass origin of the NHcX regime, the NHcT air mass type composed of several quite different air parcels and a more detailed distinction is made (Table 3).

[31] During the NHcT "Calcutta" event (DOY 64.2-65.2) the air parcels that crossed the ship track had passed the highly populated area of Calcutta (trajectory a, via F_3), and thus were influenced by combustion processes, manifested by high levels of CO, $_{18}O(CO)$, C_2H_2, CO_2, and CH_4 (Figure 2). During the NHcT "west coast" event (DOY 65.7-67.2), weaker pollution was seen as the air parcels reached the sampling site via the west coast of India (trajectory b). Ethane and propane were comparable during both periods.

4.1.2. Leg 3

[32] The trajectory-based air mass classification attributed all air masses probed during leg 3 (occurred in the Bay of Bengal) to NHmT air since the trajectories stayed over the ocean for at least 5 days before encounter. The trace gas data, however, revealed a quite high degree of pollution, CO varied between 100 and 170 ppb, and acetylene varied between 60 ppt and 150 ppt. Meteorological analyses indicated synoptical disturbances with small-scale local winds and thus less reliable back trajectories for this time. The trace gas data suggest that the air masses were imported from southeast Asia via channels F^3 (and F^4) before examination. Conclusively, all air masses during leg 3 were assigned to NHcT air (although the back trajectories suggest NHmT air).

[33] For NHcT, "high NMHC" event (DOY 87.3–88.1), compared to NHmT air, acetylene and ethane were strongly elevated concurrent with slightly enhanced levels of CO and O_3 (Tables 2 and 3), which most likely points to an aged biomass burning plume [*Mauzerall et al.*, 1998; *Singh et al.*, 2000]. A thunderstorm on early DOY 87 may have mixed several air masses, making back trajectory analysis unreliable (trajectory f).

[34] For NHcT, "low NMHC" event (DOY 88.5–88.6), a short, but sharp minimum in NMHC, O_3 (Figure 2a), and SF_6 (not shown) points to a maritime origin of this air mass, in contrast to the modestly enhanced levels of CO, CO_2, and CH_4. As only two samples are available and the trajectories changed during this time period the origin of these air masses could not be determined (trajectories g and h).

[35] For NHcT, "Bay of Bengal" event (DOY 88.9–89.3), tracers for combustion processes such as CO, $\delta^{18}O(CO)$, C_2H_2, CO_2, and CH_4 were high (Table 3), in companion with enhanced levels of other NMHCs and O_3. This again points to continental air masses imported into the Bay of Bengal by airflow F^3.

[36] In summary, the five air mass types NHcT, NHcX, NHmT, SHmT, and SHmX crossed by the *Ronald Brown* show very different mean mixing ratios of the measured compounds (Table 2). The differences between these mean values are often higher than the variance within each type of air mass which confirms the suitable identification of the individual air masses. The mixing ratios of most longer-lived compounds (CH_4, CO_2, N_2O, SF_6, ethane, propane, acetylene) and the ratio C_2H_2/CO maximized in NHcX air, followed by NHcT, NHmT, SHmT, and SHmX air. For CH_4, CO_2, N_2O, and SF_6, the longest-lived and thus the most well-mixed trace gases examined, the interhemispheric gradient is much larger than the differences between the individual types of air masses within one hemisphere. The most pronounced pollution event (DOY 67.7–75.7, in sum 8 days) was attributed to long-range transport from the extratropics, which will be analyzed in more detail now.

4.2. Influence of Meridional Long-Range Transport on the Observed Trace Gas Variability

[37] The strongly declining OH concentrations in winter toward high northern latitudes lead to a well-known accumu-

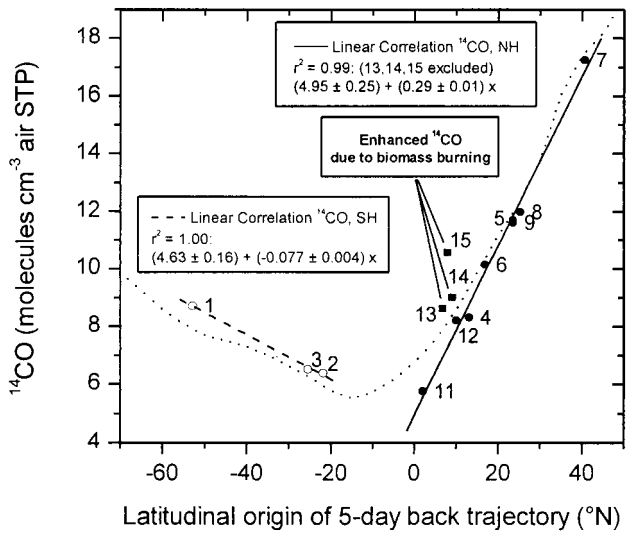

Figure 4. Concentration of ^{14}CO versus latitudinal origin of 5-day back trajectory. Linear fits for SH and NH (13,14,15 excluded) shown as dashed and solid lines, respectively. Meridional average according to a ^{14}CO climatology (based on more than 1000 measurements from 15 stations and 156 campaigns) [*Jöckel*, 2000] is shown as doted line. These data are standardized to the global average ^{14}CO production rate from 1955 to 1988 which approximately matches the production rate for 1999.

lation of various medium- and long-lived trace gases, the "NH winter plume" (hydrocarbons, CO, etc.) [*Penkett and Brice*, 1986; *Novelli et al.*, 1998; *Bonsang and Boissard*, 1999]. Strong inner NH gradients are formed for many NMHC [*Ehhalt et al.*, 1985; *Rudolph*, 1988; *Boissard et al.*, 1996], CH_4, and CO [e.g., *Novelli et al.*, 1995, 1998], which peak in late winter/early spring [*Blake and Rowland*, 1986; *Rudolph*, 1995].

[38] It is analyzed now if these strong latitudinal gradients are, at least partially, responsible for the observed trace gas variability. Carbon monoxide 14 is an ideal tracer for the latitudinal origin of an air mass, as the nature of its main source and its sink lead to a clear latitudinal gradient in ^{14}CO [*Jöckel et al.*, 1999] with weak longitudinal variations. Carbon monoxide 14 is mainly produced by a well-defined diffuse source (cosmic radiation), its production rate varies only with latitude with a minimum in the tropics (changes in solar activity and solar proton events can be disregarded). The main sink of ^{14}CO, the OH radical shows a meridional gradient with a maximum in the tropics. Typical NH background values for February-March are about 20 molecules cm^{-3} in the midlatitudes (47°N) [*Gros et al.*, 2001] and about 9 molecules cm^{-3} in the tropics (13°N) [*Mak and Southon*, 1998].

[39] During INDOEX the NH ^{14}CO concentrations (~8 to 17 molecules cm^{-3}, Figure 2b) are comparable to these values, although the latitudinal range is much smaller (~3 to 18°N), which already indicates that the observed large ^{14}CO variation is related to the different latitudinal origins. This relationship is clearly illustrated in Figure 4 (except for samples 13–15 discussed later). Carbon monoxide 14 shows a compact correlation ($r^2 \geq 0.99$) with the latitudinal origin of the 5-day back trajectories in both hemispheres. Five-day back trajectories were used, being a compromise between the declining reliability of back trajectories with time [*Stohl*, 1998] and the typical transport timescale of Rossby waves that are mostly responsible for the advection of extratropical air masses to the Indian Ocean. Moreover, an excellent agreement is found for the gradients and the values with the estimated latitudinal ^{14}CO gradient [*Jöckel*, 2000]. The foregoing reveals that the ^{14}CO variability observed during INDOEX is almost exclusively caused by long-range transport, and that the available back trajectories are reliable. Furthermore, the high ^{14}CO value of sample 7 impressively supports the extratropical origin of the air masses encountered around DOY 69.

[40] The ^{14}CO excess detected in samples 13 to 15 (leg 3) shows the impact of (^{14}C containing) biogenic CO (Figure 4), which is most probably related to biomass burning. This claim is supported by the relatively high δ^{18}O(CO) values of those three samples (Figure 2b), as well as the enhanced C_2H_2 mixing ratios. Since 10 ppb CO of biogenic origin adds 0.38 ^{14}CO molecules cm^{-3} (STP air) [*Brenninkmeijer*, 1993], the ^{14}CO excess of sample 15 would be equivalent to 85 ppb additional biogenic CO. This roughly agrees with the observed CO excess of sample 15 of ~60 ppb when assuming the observed NHmT CO mixing ratio of (92.8 ± 6.9) ppb (Table 2) as background.

[41] The successful use of the back trajectories for ^{14}CO is now applied on hydrocarbons. For this the mixing ratios of propane, ethane, and CH_4 are displayed versus the latitudinal origin of the 5-day back trajectories (Figure 5). Two regimes become visible. First, low mixing ratios and no significant correlation with latitude south of ~16°N, in particular obvious for propane that is <25 ppt south of ~16°N, representing background conditions. Second, progressively increasing mixing ratios with latitude north of ~16°N. This confirms that the observed trace gas variability primarily reflects the latitudinally varying origin of the sampled air masses and that 16°N is about the border between regions recently influenced by continental outflow and more pristine areas.

[42] Moreover, it demonstrates that long-range advection from the extratropical NH strongly contributes to the pollution of the Indian Ocean (at least during INDOEX) and that a significant fraction of the "NH winter plume" is decomposed at lower latitudes, in agreement with model results [*Gupta et al.*, 1998]. Nevertheless, this finding does not imply that the extratropical NH is the major source of pollution to the Indian Ocean (via F^2). Severe pollution from local sources, especially from the Calcutta region, was intersected near the tip of India while F^3 was active (DOY 58–59, 64–65) and (as already noted) F^3 and F^4 are usually more persistent. Additionally, these recent air masses are expected to be rich in NO_x (in contrast to aged NHcX air) which is required to generate O_3.

[43] Worth mentioning is that the latitudinal CH_4 gradient of (1.7 ± 0.2) ppb / °N (r^2 = 0.66, except samples south of the chemical ITCZ, Figure 5) agrees reasonably with ~2.2 ppb/ °N and ~1.9 ppb / °N extracted from several latitudinal distributions (annual means, 1984–1993) [*Dlugokencky et al.*, 1994] and retrieved from NOAA/CMDL data for March, 1999.

4.3. Discussion of the Use of the C_2H_2/CO Ratio As a Measure for Atmospheric Processing

[44] Acetylene and CO have comparable atmospheric cycles. Both are largely combustion products and are removed by the reaction with OH. Owing to the difference in lifetime against OH (for C_2H_2 ~1/3 of that of CO, Table 1) photochemical aging of an air mass after its emissions leads to decreasing C_2H_2/CO ratios. A competing process also leading to a decrease of the C_2H_2/CO ratio is mixing. Thus C_2H_2/CO

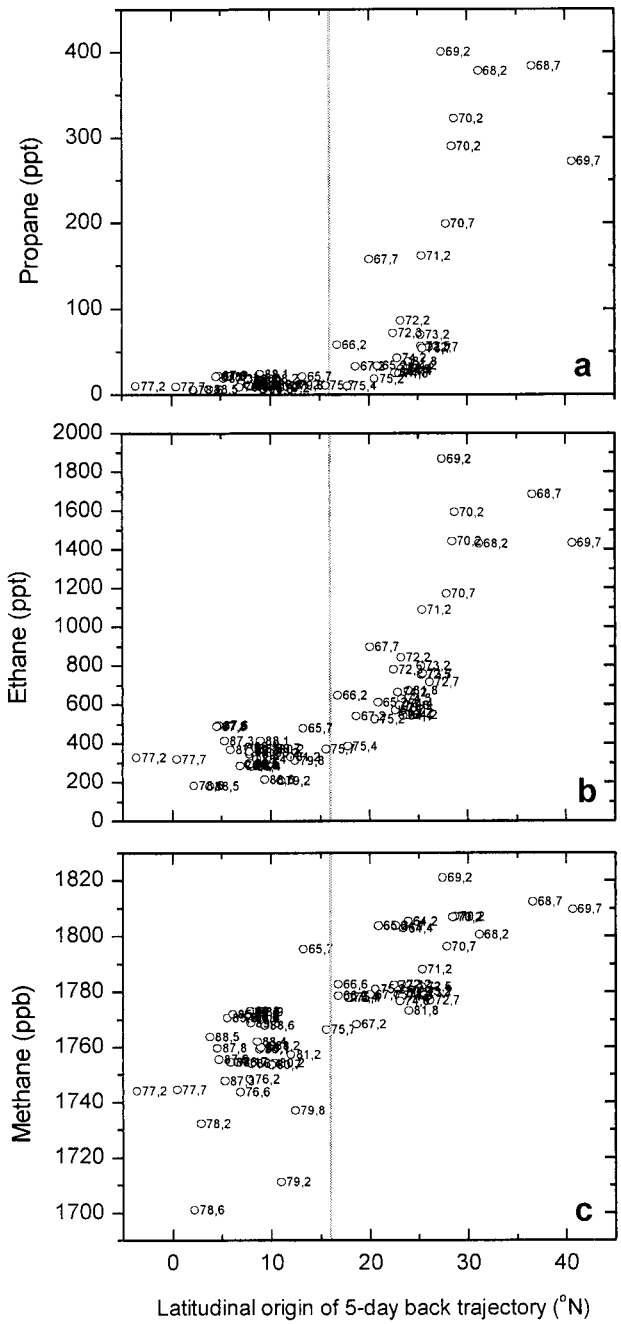

Figure 5. Mixing ratios of (a) propane, (b) ethane, and (c) methane versus latitudinal origin of 5-day back trajectory, divided up in north of ~16°N and south of ~16°N (see section 4.2). Days of year (DOY) are noted.

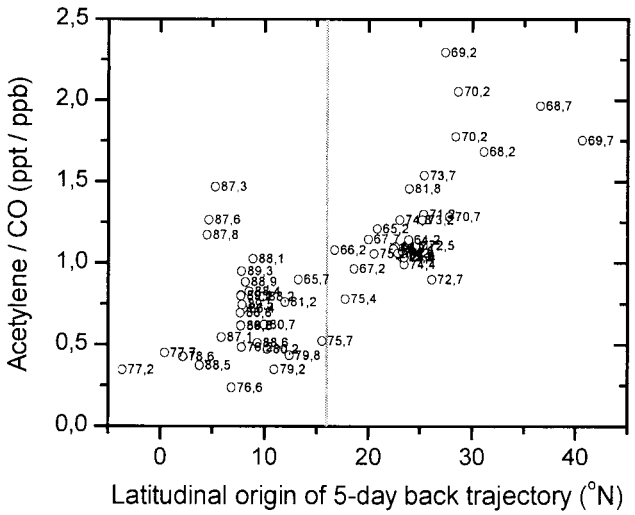

Figure 6. Ratio of acetylene to carbon monoxide (ppt/ppb) versus latitudinal origin of 5-day back trajectory, divided up in north of ~16°N and south of ~16°N. Days of year (DOY) are noted.

contains information on the sum of mixing and photochemistry ("atmospheric processing") [*McKeen and Liu*, 1993]. Note that local sources or mixing with different air masses corrupt the C_2H_2/CO ratio.

[45] On the basis of this tool, *Smyth et al.* [1996, 1999] concluded that "mixing" strongly dominated over "chemistry" during the Pacific Exploratory Missions (PEM) in the free atmosphere. Rapidly decreasing C_2H_2/CO ratios with a half-lifetime of typically 1–3 days were recorded, which primarily reflected the speed of mixing with background air.

[46] It is demonstrated now that the information derived from the C_2H_2/CO ratio differs strongly from the results by *Smyth et al.* [1996, 1999] when applied to the measurements over the Indian Ocean. As seen in Figure 2, maximum C_2H_2/CO ratios of up to 2.3 ppt/ppb were encountered in air masses that originated from the extratropical free troposphere (around DOY 69) and subsided to the marine boundary layer near the coastline. According to *Smyth et al.* [1999] such C_2H_2/CO ratios should mark air mass ages of <2 days, which seems to be unrealistic as the back trajectories show that the "source area" is more than 5 days away. The following conditions encountered during INDOEX and the PEM missions are different.

1. In the extratropical NH winter/early spring, C_2H_2 strongly accumulates (see section 4.2), so that the C_2H_2/CO background ratio is much higher than in the free troposphere over the Pacific (<0.5 ppt/ppb). Therefore mixing with background air has a smaller impact on the decline of the C_2H_2/CO ratio compared to the free troposphere over the Pacific. This claim is supported by observations by *Roths and Harris* [1996] and *Boissard et al.* [1996], who found 100–130 ppb CO and 300–400 ppt C_2H_2, respectively, in the free troposphere at 30°–45°N in January (Tropospheric Ozone Experiment (TROPOZ) II), which corresponds to a C_2H_2/CO ratio of ~3 ppt/ppb. These contrasting conditions are reflected in the INDOEX data (Figure 6). Indeed, the air masses with the highest C_2H_2/CO ratios originate from the extratropics (see NHcX, Table 2, Figure 2a) where the C_2H_2/CO background ratio is much higher than in the tropics.

2. Mixing with background air is reduced in the planetary boundary layer compared to the free troposphere, which slows down the decrease of the C_2H_2/CO ratio with time. Note that *Smyth et al.* [1996, 1999] have omitted the measurements made in the boundary layer from their analysis.

[47] Conclusively, the C_2H_2/CO ratio during INDOEX was less affected by mixing compared to the free troposphere over the Pacific (i.e., during the PEM missions), where mixing was found to be the dominant effect influencing the C_2H_2/CO ratio. Therefore the relationship between the C_2H_2/CO ratio and air mass age given by *Smyth et al.* [1996, 1999] which is

Table 4. Mixing Ratios (Mean and 1 σ Variation) at Altitudes <2 km During PEM-West B (February-March 1994)[a]

Type of Air Mass	Continental-North Outflow (<2 Days)	Continental-South Outflow (<2 Days)	Aged Marine (>5 Days)
CH_4,[b] ppb	1810 ± 24	1756 ± 12	1722 ± 31
CO_2,[b] ppb	364.0 ± 2.5	359.9 ± 1.5	358.5 ± 0.8
N_2O, ppb	312.0 ± 0.39	-	-
SF_6, ppt	-	-	-
Ethane, ppt	2337 ± 377	1063 ± 219	525 ± 212
Propane, ppt	961 ± 314	125 ± 56	44 ± 17
Acetylene, ppt	908 ± 356	458 ± 177	72 ± 38
C_2H_2/CO, ppt/ppb	4.4 ± 0.67	2.4 ± 0.55	2.1 ± 2.4
CO, ppb	206 ± 68	182 ± 37	92 ± 16
O_3, ppb	44 ± 9	39 ± 15	18 ± 6

[a]From *Talbot et al.* [1997].
[b]CO_2 and CH_4 increased from 1994 to 1999 by ~10 ppm and 31 ppb, respectively (global, NOAA/CMDL).

based on the dominance of mixing is not applicable during INDOEX for air masses advected from latitudes north of ~16°N.

[48] Note that in areas which were not recently affected by extratropical air masses (south of ~16°N), enhanced C_2H_2/CO ratios of up to 1.5 (on DOY 87), the "high NMHC" event (Table 3, Figure 2a), were related to an aged biomass burning plume (section 4.1.2, second paragraph). However, compared to PEM-West B, the C_2H_2/CO ratios were much lower (Table 4), which demonstrates that the air masses intersected by the R/V *Ronald Brown* were less affected by fresh emissions from combustion processes, which is supported by other trace gas data (see section 5).

5. Comparison With Previous Observations

[49] Compared to the pre-INDOEX ship study by *Rhoads et al.* [1997] (March-April 1995), more severe pollution was encountered during INDOEX in NH air masses, supported, among others, by the higher mixing ratios of CO and O_3 [*Stehr et al.*, 2002]. Tracers for combustion (see Table 1) peaked in the Arabian Sea (in agreement with *Lal et al.* [1998] and *Naja et al.* [1999]) and the Bay of Bengal, both areas not visited by *Rhoads et al.* [1997]. These regions are surrounded by densely populated areas and are affected by advection from the extratropics. *Rhoads et al.* [1997] found two SH maritime regimes, based on a rise of CO and non-sea salt aerosol (but without a corresponding change in the back trajectories). The INDOEX trace gas data and the back trajectory calculations support the presence of two SH air mass types (SHmT and SHmX), see Table 2. The INDOEX data confirm the distinction in meteorological regimes made by *Rhoads et al.* [1997] and W. P. Ball et al. (unpublished manuscript, 2002) and give further evidence for the importance of transport of anthropogenic emissions to the remote Indian Ocean.

[50] Ethane and acetylene mixing ratios in the NHcX regime are comparable to previous marine springtime measurements in the tropics/subtropics [*Rudolph and Ehhalt*, 1981; *Rudolph and Johnen*, 1990; *Atlas et al.*, 1993; *Donahue and Prinn*, 1993] and in the free troposphere at 30°–40°N (1–2 ppb and 0.2–0.5 ppb, respectively) [*Boissard et al.*, 1996], which supports the importance of advection from the extratropical NH. *Bonsang et al.* [1988] reported similar ethane values in coastal vicinity of Africa, but acetylene remained much lower (<30 ppt). Propane values are similar to several reports [*Rudolph and Ehhalt*, 1981; *Bonsang et al.*, 1988; *Rudolph and Johnen*, 1990; *Atlas et al.*, 1993; *Donahue and Prinn*, 1993].

[51] Numerous NHcT and most NHmT propane measurements are at the lower end of previous reports, which emphasizes the remote character already seen at the back trajectories. Only *Rudolph and Johnen* [1990] and *Atlas et al.* [1993] reported comparable low propane mixing ratios.

[52] The mixing ratios of ethane and acetylene in SHmT air are in the range of previous observations in the southern Indian Ocean [*Kanakidou et al.*, 1988; *Bonsang et al.*, 1990; *Touaty et al.*, 1996] and other tropical Ocean sites [*Blake and Rowland*, 1986; *Rudolph and Johnen*, 1990] in late winter/early spring. *Rudolph* [1995] retrieved ~270–300 ppt ethane from a database for February with a gradual transition from NH to SH. As pointed out by *Rudolph* [1995], this difference to the stepwise change observed by *Donahue and Prinn* [1993] (as well as during INDOEX, Figure 2a, DOY 79), is the result of averaging. Due to the variable location of the chemical ITCZ (south or north of the equator), the sharp drop is smoothed out in the longitudinally averaged latitudinal profile given by *Rudolph* [1995]. *Saito et al.* [2000] reported 3–6 times higher acetylene values in the Indian Ocean, probably due to the encounter of strong pollution. Comparable propane levels were observed in the remote Atlantic ocean [*Rudolph and Johnen*, 1990].

[53] During PEM-West B (February-March, 1994) where the Asian outflow to the Pacific Ocean was analyzed, distinctly higher concentrations of pollutants were encountered below 2 km altitude [*Blake et al., 1997*; *Talbot et al.*, 1997]. All trace gases except CO_2 were significantly higher (Table 4) in continentally influenced air masses (origin >20°N, classified by *Talbot et al.* [1997] as continental north). Compared to the fresh continental outflow encountered during PEM below 5 km altitude, the air masses sampled by the *Ronald Brown* were aged, i.e., had no contact with landmasses for more than 4 days. Even less polluted air masses classified by *Talbot et al.* [1997] as continental south (origin <20°N) showed higher levels of typical pollution tracers, e.g., CO and acetylene. Aged marine masses [*Talbot et al.*, 1997] and NHmT air during INDOEX had a more comparable trace gas composition (Table 4) (except for propane), but the slightly higher acetylene and ethane mixing ratios document a less pristine character even for the aged maritime air.

6. Conclusions

[54] During the INDOEX R/V *Ronald Brown* cruise in the Indian Ocean (February-March 1999, track in Figure 1), pronounced variability in various medium- and long-lived trace gases, such as NMHC, CH_4, CO, and CO_2, was observed. This variability was partially related to nearby continental outflow from India and Southeast Asia via the airflows F^3 and F^4 (the four prevailing airflows are shown in Figure 1), but the strongest pollution event was caused by long-range transport from the extratropical NH (Middle East and probably even Europe) via airflow F^2. In comparison to the PEM-West B expedition over the Pacific Ocean (February-March 1994), little fresh pollution was encountered by the R/V *Ronald Brown*; most air masses had no contact with landmasses for more than 4 days. Because of the atypical meteorological situation during INDOEX [*Verver et al.,* 2001], it can be expected that the continental outflow from India and Southeast Asia via F^3 and F^4 is usually more persistent in the lower troposphere. Note that throughout the INDOEX campaign layers of fresh pollution were actually encountered, but mainly above the marine boundary layer (MBL), demonstrated by extensive airborne trace gas and aerosol measurements [*Mayol-Bracero et al.*, 2002, *Sheridan et al.*, 2002].

[55] The presence of long-range advection of pollutants in the Indian Ocean was excellently confirmed by the measured ^{14}CO. Using 5-day back trajectories, a compact latitudinal gradient ($r^2 \geq 0.99$) of (0.29 ± 0.01) molecules cm^{-3}/°N in the NH and (0.077 ± 0.004) molecules cm^{-3}/°S in the SH was inferred, in excellent agreement with the ^{14}CO climatology by *Jöckel* [2000].

[56] For air masses that were imported from latitudes north of ~16°N, the C_2H_2/CO ratio was found to be unsuitable as a measure for atmospheric processing as defined by *Smyth et al.*, [1996, 1999] for the PEM missions. This difference is caused by the lower impact of mixing during INDOEX compared to PEM, where mixing was found to be the dominant effect influencing the C_2H_2/CO ratio. First, due to the strong accumulation of pollutants in the winter northern hemisphere and the corresponding elevated background C_2H_2/CO ratio of typically 3 ppt/ppb (much higher than the ~0.5 ppt/ppb during PEM-West B), the impact of mixing on the C_2H_2/CO ratio is reduced. Second, mixing with background air in the marine boundary layer is small compared to the free troposphere. Therefore elevated C_2H_2/CO ratios during INDOEX mostly reflected import of air masses from the extratropics. However, south of ~16°N enhanced C_2H_2/CO ratios, as observed in the Bay of Bengal, could be assigned to biomass burning, supported by other NMHC as well as the $^{14}C/^{12}C$ and $^{18}O/^{16}O$ isotope ratios of CO.

[57] **Acknowledgments.** The work was supported by the BMBF under the grant 01LA9831/2. We thank J. E. Johnson and J. W. Stehr for provision of the CO and O_3 data, and the National Oceanic and Atmospheric Administration (NOAA) Climate Monitoring and Diagnostics Laboratory (CMDL) Carbon Cycle Group for reference data on CH_4, CO, and CO_2. We are grateful to R. Hofmann, W. Hanewacker, C. Koeppel, and R. Schmunck for their careful analyses. We especially thank the two anonymous reviewers for their valuable comments on the manuscript.

References

Apel, E. C., and J. G. Calvert, Initial results from the nonmethane hydrocarbon intercomparison experiment, *J. Chin. Chem. Soc., 41,* 279–286, 1994.

Apel, E. C., J. G. Calvert, and F. C. Fehsenfeld, The nonmethane hydrocarbon intercomparison experiment (NOMHICE): Tasks 1 and 2, *J. Geophys. Res., 99,* 16,651–16,664, 1994.

Apel, E. C., J. G. Calvert, T. M. Gilpin, F. C. Fehsenfeld, D. D. Parrish, and W. A. Lonneman, The nonmethane hydrocarbon intercomparison experiment (NOMHICE): Task 3, *J. Geophys. Res., 104,* 26,069–26,086, 1999.

Arlander, D. W., D. R. Cronn, J. C. Farmer, F. A. Menzia, and H. H. Westberg, Gaseous oxygenated hydrocarbons in the remote marine troposphere, *J. Geophys. Res., 95,* 16,391–16,403, 1990.

Atlas, E., W. Pollock, J. Greenberg, L. Heidt, and A. M. Thompson, Alkyl nitrates, nonmethane hydrocarbons, and halocarbon gases over the equatorial Pacific Ocean during SAGA 3, *J. Geophys. Res., 98,* 16,933–16,947, 1993.

Baldy, S., G. Ancellet, M. Bessafi, A. Badr, and D. L. S. Luk, Field observations of the vertical distribution of tropospheric ozone at the Island of Reunion (southern tropics), *J. Geophys. Res., 101,* 23,835–23,849, 1996.

Bange, H. W., S. Rapsomanikis, and M. O. Andreae, Nitrous oxide emissions from the Arabian Sea, *Geophys. Res. Lett., 23,* 3175–3178, 1996.

Bange, H. W., R. Ramesh, S. Rapsomanikis, and M. O. Andreae, Methane in surface waters of the Arabian Sea, *Geophys. Res. Lett., 25,* 3547–3550, 1998.

Blake, D. R., and F. S. Rowland, Global atmospheric concentrations and source strength of ethane, *Nature, 321,* 231–233, 1986.

Blake, N. J., D. R. Blake, T. Y. Chen, J. E. Collins, G. W. Sachse, B. E. Anderson, and F. S. Rowland, Distribution and seasonality of selected hydrocarbons and halocarbons over the western Pacific basin during PEM-West A and PEM-West B, *J. Geophys. Res., 102,* 28,315–28,331, 1997.

Boissard, C., B. Bonsang, M. Kanakidou, and G. Lambert, Tropoz II - Global distributions and budgets of methane and light hydrocarbons, *J. Atmos. Chem., 25,* 115–148, 1996.

Bonsang, B., and C. Boissard, Global distribution of reactive hydrocarbons in the atmosphere, in *Reactive Hydrocarbons in the Atmosphere,* pp. 209–265, Academic, San Diego, Calif., 1999.

Bonsang, B., M. Kanakidou, G. Lambert, and P. Monfray, The marine source of C_2-C_6 aliphatic hydrocarbons, *J. Atmos. Chem., 6,* 3–20, 1988.

Bonsang, B., M. Kanakidou, and G. Lambert, NMHC in the marine atmosphere: Preliminary results of monitoring at Amsterdam Island, *J. Atmos. Chem., 11,* 169–178, 1990.

Bonsang, B., C. Polle, and G. Lambert, Production of non-methane hydrocarbons by seawater, *Ann. Inst. Óceanogr., 69,* 125–128, 1993.

Bräunlich, M., Study of the atmospheric carbon monoxide and methane using isotopic analysis, dissertation thesis, Rupertus Carola Univ., Heidelberg, Germany, 2000.

Brenninkmeijer, C. A. M., Measurement of the abundance of ^{14}CO in the atmosphere and the $^{13}C/^{12}C$ and $^{18}O/^{16}O$ ratio of atmospheric CO, with application in New-Zealand and Antarctica, *J. Geophys. Res., 98,* 10,595–10,614, 1993.

Brenninkmeijer, C. A. M., T. Röckmann, M. Bräunlich, P. Jöckel, and P. Bergamaschi, Review of progress in isotope studies of atmospheric carbon monoxide, *Chemosphere Global Change Sci., 1,* 33–52, 1999.

Brenninkmeijer, C. A. M., C. Koeppel, T. Röckmann, D. S. Scharffe, M. Bräunlich, and V. Gros, Absolute measurement of the abundance of atmospheric carbon monoxide, *J. Geophys. Res., 106,* 10,003–10,010, 2001.

Butler, J. H., J. W. Elkins, C. M. Brunson, K. B. Egan, T. M. Thompson, T. J. Conway, and B. D. Hall, Trace gases in and over the West Pacific and East Indian Oceans during the El Nino-Southern Oscillation event of 1987, *NOAA Rep. ERL ARL-16,* Natl. Oceanic and Atmos. Admin., Boulder, Colo., 1988.

Camel, V., and M. Caude, Trace enrichment methods for the determination of organic pollutants in ambient air, *J. Chromatogr. A, 710,* 3–19, 1995.

de Laat, A. T. J., M. Zachariasse, G. J. Roelofs, P. van Velthoven, R. R. Dickerson, K. P. Rhoads, S. J. Oltmans, and J. Lelieveld, Tropospheric O_3 distribution over the Indian Ocean during spring 1995 evaluated with a chemistry-climate model, *J. Geophys. Res., 104,* 13,881–13,893, 1999.

DeMore, W. B., S. P. Sander, D. M. Golden, R. F. Hampson, M. J. Kurylo, C. J. Howard, A. R. Ravishankara, C. E. Kolb, and M. J.

Molina, Chemical kinetics and photochemical data for use in stratospheric modeling, *Evaluation 12, JPL Publ., 97-4,* 1997.

Dlugokencky, E. J., L. P. Steele, P. M. Lang, and K. A. Masarie, The growth-rate and distribution of atmospheric methane, *J. Geophys. Res., 99,* 17,021–17,043, 1994.

Donahue, N. M., and R. G. Prinn, In situ nonmethane hydrocarbon measurements on SAGA 3, *J. Geophys. Res., 98,* 16,915–16,932, 1993.

Doskey, P. V., The effect of treating air samples with magnesium perchlorate for water removal during analysis for non-methane hydrocarbons, *J. High Resolut. Chromatogr., 14,* 724–728, 1991.

Doskey, P. V., J. A. Porter, and P. A. Scheff, Source fingerprints for non-volatile hydrocarbons, *J. Air Waste Manage. Assoc., 42,* 1437–1445, 1992.

Draxler, R. R., and G. D. Hess, An overview of the HYSPLIT_4 modelling system for trajectories, dispersion, and deposition, *Aust. Meteorol. Mag., 47,* 295–308, 1998.

Ehhalt, D. H., J. Rudoplh, F. X. Meixner, and U. Schmidt, Measurements of selected C_2-C_5 hydrocarbons in the background troposphere: vertical and latitudinal variations, *J. Atmos. Chem., 3,* 29–52, 1985.

Goyet, C., F. J. Millero, D. W. Osullivan, G. Eischeid, S. J. McCue, and R. G. J. Bellerby, Temporal variations of Pco(2) in surface seawater of the Arabian Sea in 1995, *Deep Sea Res., Part I, 45,* 609–623, 1998.

Gros, V., N. Poisson, D. Martin, M. Kanakidou, and B. Bonsang, Observations and modeling of the seasonal variation of surface ozone at Amsterdam Island: 1994–1996, *J. Geophys. Res., 103,* 28,103–28,109, 1998.

Gros, V., et al., Detailed analysis of the isotopic composition of CO and characterization of air masses arriving at Mount Sonnblick (Austrian Alps), *J. Geophys. Res., 106,* 3179–3193, 2001.

Gupta, M. L., R. J. Cicerone, D. R. Blake, F. S. Rowland, and I. S. A. Isaksen, Global atmospheric distributions and source strengths of light hydrocarbons and tetrachloroethene, *J. Geophys. Res., 103,* 28,219–28,235, 1998.

Habram, M., J. Slemr, and T. Welsch, Development of a dual capillary column GC method for the trace determination of C_2-C_9 hydrocarbons in ambient air, *J. High Resolut. Chromatogr., 21,* 209–214, 1998.

Helmig, D., Air analysis by gas chromatography, *J. Chromatogr. A, 843,* 129–146, 1999.

Hough, A. M., Development of a two-dimensional global tropospheric model: Model chemistry, *J. Geophys. Res., 96,* 7325–7362, 1991.

Intergovernmental Panel on Climate Change (IPCC), *Climate Change 1994: Radiative Forcing of Climate Change and an Evaluation of the IPCC IS 92 Emissions Scenarios,* edited by J. T. Houghton et al., 339 pp., Cambridge Univ. Press, New York, 1995

Jöckel, P., Cosmogenic ^{14}CO as tracer for atmospheric chemistry and transport, dissertation thesis, Rupertus Carola Univ., Heidelberg, Germany, 2000.

Jöckel, P., M. G. Lawrence, and C. A. M. Brenninkmeijer, Simulations of cosmogenic ^{14}CO using the three-dimensional atmospheric model MATCH: Effects of ^{14}C production distribution and the solar cycle, *J. Geophys. Res., 104,* 11,733–11,743, 1999.

Johnson, J. E., R. H. Gammon, J. Larsen, T. S. Bates, S. J. Oltmans, and J. C. Farmer, Ozone in the marine boundary layer over the Pacific and Indian Oceans: Latitudinal gradients and diurnal cycles, *J. Geophys. Res., 95,* 11,847–11,856, 1990.

Kanakidou, M., B. Bonsang, J. C. Le Roulley, G. Lambert, D. Martin, and G. Sennequier, Marine source of atmospheric acetylene, *Nature, 333,* 51–52, 1988.

Kurdziel, M., The effect of different drying agents on the analytical data for non-methane hydrocarbon concentrations in ambient air samples, *Chem. Anal. (Warsaw), 43,* 387–397, 1998.

Lal, S., M. Naja, and A. Jayaraman, Ozone in the marine boundary layer over the tropical Indian Ocean, *J. Geophys. Res., 103,* 18,907–18,917, 1998.

Lewis, A. C., J. B. McQuaid, N. Carslaw, and M. J. Pilling, Diurnal cycles of short-lived tropospheric alkenes at a north Atlantic coastal site, *Atmos. Environ., 33,* 2417–2422, 1999.

Maiss, M., L. P. Steele, R. J. Francey, P. J. Fraser, R. L. Langenfelds, N. B. A. Trivett, and I. Levin, Sulfur hexafluoride - A powerful new atmospheric tracer, *Atmos. Environ., 30,* 1621–1629, 1996.

Mak, J. E., and C. A. M. Brenninkmeijer, Compressed air sample technology for isotopic analysis of atmospheric carbon monoxide, *J. Atmos. Oceanic Technol., 11,* 425–431, 1994.

Mak, J. E., and J. R. Southon, Assessment of tropical OH seasonality using atmospheric ^{14}CO measurements from Barbados, *Geophys. Res. Lett., 25,* 2801–2804, 1998.

Matuška, P., M. Koval, and W. Seiler, A high resolution GC-analysis method for determination of C_2-C_{10} hydrocarbons in air samples, *J. High Resolut. Chromatogr. Chromatogr. Commun., 9,* 577–583, 1986.

Mauzerall, D. L., J. A. Logan, D. J. Jacob, B. E. Anderson, D. R. Blake, J. D. Bradshaw, B. Heikes, G. W. Sachse, H. Singh, and B. Talbot, Photochemistry in biomass burning plumes and implications for tropospheric ozone over the tropical South Atlantic, *J. Geophys. Res., 103,* 8401–8423, 1998.

Mayol-Bracero, O. L., T. W. Kirchstetter, T. Novakov, M. O. Andreae, R. Gabriel, and D. G. Streets, Carbonaceous aerosols over the Indian Ocean during INDOEX: Chemical characterization, optical properties, and probable sources, *J. Geophys. Res., 107*(DX), 10.1029/2000JD000039, in press, 2002.

McKeen, S. A., and S. C. Liu, Hydrocarbon ratios and photochemical history of air masses, *Geophys. Res. Lett., 20,* 2363–2366, 1993.

Mitra, A. P., INDOEX (India): Introductory note, *Curr. Sci., 76,* 886–889, 1999.

Mitra, S., and C. Yun, Continuous gas chromatographic monitoring of low concentration sample streams using an on-line microtrap, *J. Chromatogr., 648,* 415–421, 1993.

Naja, M., S. Lal, S. Venkataramani, K. S. Modh, and D. Chand, Variabilities in O_3, NO, CO and CH_4 over the Indian Ocean during winter, *Curr. Sci., 76,* 931–937, 1999.

Novelli, P. C., T. J. Conway, E. J. Dlugokency, and P. P. Tans, Recent changes in atmospheric carbon dioxide, methane and carbon monoxide, and the implications of these changes on global climate, *WMO Bull., 44,* 32–37, 1995.

Novelli, P. C., K. A. Masarie, and P. M. Lang, Distributions and recent changes of carbon monoxide in the lower troposphere, *J. Geophys. Res., 103,* 19,015–19,033, 1998.

Penkett, S. A., and K. A. Brice, The spring maximum in photo-oxidants in the Northern Hemisphere troposphere, *Nature, 319,* 655–657, 1986.

Plass-Dülmer, C., R. Koppmann, M. Ratte, and J. Rudolph, Light nonmethane hydrocarbons in seawater, *Global Biogeochem. Cycles, 9,* 79–100, 1995.

Rasmussen, R. A., C. W. Lewis, R. K. Stevens, W. D. Ellenson, and S. L. Dattner, Removing CO_2 from atmospheric samples for radiocarbon measurements of volatile compounds, *Environ. Sci. Technol., 30,* 1092–1097, 1996.

Rhoads, K. P., P. Kelley, R. R. Dickerson, T. P. Carsey, M. Farmer, D. L. Savoie, and J. M. Prospero, Composition of the troposphere over the Indian Ocean during the monsoonal transition, *J. Geophys. Res., 102,* 18,981–18,996, 1997.

Roths, J., and G. W. Harris, The tropospheric distribution of carbon monoxide as observed during the TROPOZ II experiment, *J. Atmos. Chem., 24,* 157–188, 1996.

Rudolph, J., Two-dimensional distribution of light hydrocarbons: Results from the STRATOZ III experiment, *J. Geophys. Res., 93,* 8367–8377, 1988.

Rudolph, J., The tropospheric distribution and budget of ethane, *J. Geophys. Res., 100,* 11,369–11,381, 1995.

Rudolph, J., and D. H. Ehhalt, Measurements of C_2-C_5 hydrocarbons over the North Atlantic, *J. Geophys. Res., 86,* 11,959–11,964, 1981.

Rudolph, J., and F. J. Johnen, Measurements of light atmospheric hydrocarbons over the Atlantic in regions of low biological activity, *J. Geophys. Res., 95,* 20,583–20,591, 1990.

Rudolph, J., F. J. Johnen, A. Khedim, and G. Pilwat, The use of automated "on line" gaschromatography for the monitoring of organic trace gases in the atmosphere at low levels, *Int. J. Environ. Anal. Chem., 38,* 143–155, 1990.

Rudolph, J., R. Koppmann, and C. Plass-Dülmer, The budgets of ethane and tetrachloroethene - Is there evidence for an impact of reactions with chlorine atoms in the troposphere, *Atmos. Environ., 30,* 1887–1894, 1996.

Saito, T., Y. Yokouchi, and K. Kawamura, Distributions of C_2-C_6 hydrocarbons over the western North Pacific and eastern Indian Ocean, *Atmos. Environ., 34,* 4373–4381, 2000.

Sheridan, P., A. Jefferson, and J. Ogren, Spatial variability of aerosol radiative properties over the Indian Ocean during INDOEX, *J. Geophys. Res., 107*(DX), 10.1029/2000JD000166, in press, 2002.

Singh, H. B., and P. B. Zimmerman, Atmospheric distribution and sources of nonmethane hydrocarbons, in *Advances in Environmental*

Science & Technology, edited by J. O. Nriagu, pp. 177–235, John Wiley, New York, 1992.

Singh, H. B., W. Viezee, and L. J. Salas, Measurements of selected C_2-C_5 hydrocarbons in the troposphere: Latitudinal, vertical, and temporal variations, *J. Geophys. Res., 93,* 15,861–15,878, 1988.

Singh, H. B., et al., Biomass burning influences on the composition of the remote South Pacific troposphere: Analysis based on observations from PEM-Tropics-A, *Atmos. Environ., 34,* 635–644, 2000.

Smyth, S., et al., Comparison of free tropospheric western Pacific air mass classification schemes for the PEM-West A experiment, *J. Geophys. Res., 101,* 1743–1762, 1996.

Smyth, S., et al., Characterization of the chemical signatures of air masses observed during the PEM experiments over the western Pacific, *J. Geophys. Res., 104,* 16,243–16,254, 1999.

Stehr, J. W., W. P. Ball, R. R. Dickerson, B. G. Doddridge, C. Piety, and J. E. Johnson, Latitudinal gradients in O_3 and CO during INDOEX 1999, *J. Geophys. Res., 107*(DX), 10.1029/2001JD000446, in press, 2002.

Stohl, A., Computation, accuracy and applications of trajectories - A review and bibliography, *Atmos. Environ., 32,* 947–966, 1998.

Talbot, R. W., et al., Chemical characteristics of continental outflow from Asia to the troposphere over the western Pacific Ocean during February-March 1994: Results from PEM-West B, *J. Geophys. Res., 102,* 28,255–28,274, 1997.

Taupin, F. G., M. Bessafi, S. Baldy, and P. J. Bremaud, Tropospheric ozone above the southwestern Indian Ocean is strongly linked to dynamical conditions prevailing in the tropics, *J. Geophys. Res., 104,* 8057–8066, 1999.

Touaty, M., B. Bonsang, M. Kanakidou, and N. Poisson, Monitoring and model comparison of the seasonal variation of tropospheric light hydrocarbons at Amsterdam Island, in *Proceedings of EUROTRAC Symposium,* edited by P. M. Borrell et al., pp. 613–619, Comput. Mech., Billerica, Mass., 1996.

Upstill-Goddard, R. C., J. Barnes, and N. J. P. Owens, Nitrous oxide and methane during the 1994 SW monsoon in the Arabian Sea/northwestern Indian Ocean, *J. Geophys. Res., 104,* 30,067–30,084, 1999.

Verver, G. H. L., D. R. Sikka, J. M. Lobert, G. Stossmeister, and M. Zachariasse, Overview of the meteorological conditions and atmospheric transport processes during INDOEX 1999, *J. Geophys. Res., 106,* 28,399–28,413, 2001.

Wisthaler, A., A. Hansel, R. R. Dickerson, and P. J. Crutzen, Organic trace gas measurements by PTRMS during INDOEX 1999, *J. Geophys. Res., 107*(DX), 10.1029/2001JD000576, in press, 2002.

C. A. M. Brenninkmeijer, P. J. Crutzen, V. Gros, J. Mühle, and A. Zahn, Air Chemistry Division, Max Planck Institute for Chemistry, P.O. Box 3060, 55020 Mainz, Germany. (muehle@mpch-mainz.mpg.de)